Exploring the Proline-Dependent Conformational Change in the Multifunctional PutA Flavoprotein by Tryptophan Fluorescence Spectroscopy†

Weidong Zhu and Donald F. Becker*

Department of Biochemistry, Redox Biology Center, University of Nebraska, Lincoln, Nebraska 68588

Received May 31, 2005; Revised Manuscript Received July 25, 2005

ABSTRACT: The multifunctional PutA flavoprotein regulates proline utilization in *Escherichia coli* by switching from a cytosolic DNA-binding protein to a membrane-bound enzyme with proline dehydrogenase (PRODH) and Δ^1-pyrroline-5-carboxylate dehydrogenase (P5CDH) activities. The transformation of PutA from a transcriptional repressor of the proline utilization (*put*) regulon to a peripheral membrane associated enzyme is mediated by a proline-dependent conformational change. Previously, limited proteolysis of PutA indicated that the conformational change involves a flexible domain of unknown function (residues 141−262) which is nearby the FAD-binding and PRODH active sites (residues 263−610). Here, we extend our understanding of the proline-dependent conformational change in PutA by investigating the intrinsic Trp fluorescence spectroscopic properties of a truncated PutA protein which contains residues 86−601 (PutA86−601) and only four Trp residues. The addition of proline to wild-type PutA86−601 decreases Trp fluorescence by 36%, indicating a substantial conformational change. An apparent rate constant of 0.59 ± 0.06 s^{-1} was determined for the fluorescence change by stopped-flow fluorescence measurements. The limiting rate constant for proline reduction of the FAD cofactor in PutA is 133 ± 6 s^{-1}, demonstrating that FAD reduction precedes the conformational transition observed by Trp fluorescence. The nonreducing ligand L-tetrahydro-2-furoic acid mimics the decrease in Trp fluorescence induced by proline, indicating that both FAD reduction and ligand binding contribute to the observed conformational change in PutA86−601. W194 and W211, which are located in the flexible domain, were replaced by Phe in the PutA86−601 mutants W194F, W211F, and W194F/W211F to determine which residue is involved in the observed fluorescence change. Analysis of the PutA86−601 mutants indicated that W211 is the primary molecular marker of the conformational change caused by proline. Altogether, this work shows that the switching of PutA from a transcriptional repressor to a membrane-bound protein involves W211 in a flexible domain near the PRODH active site and occurs on a time scale that is >10-fold slower than the turnover number of PutA.

The catabolism of proline to glutamate in Gram-negative bacteria such as *Escherichia coli* and *Salmonella typhimurium* depends on the multifunctional PutA (proline utilization A) flavoenzyme which has two catalytic functions. The enzymatic functions are performed by discrete proline dehydrogenase (PRODH)[1] and P5C dehydrogenase (P5CDH) domains in PutA. The dehydrogenation of proline to P5C in the PRODH active site involves reductive and oxidative half-reactions. In the reductive half-reaction two electrons from proline are transferred to the FAD cofactor, while in the oxidative half-reaction two electrons are transferred from reduced FAD to an acceptor in the electron transport chain. Thus, PutA is peripherally membrane associated during proline oxidation (*1*). Following the hydrolysis of P5C to γ-glutamic acid semialdehyde (GSA), the P5CDH domain catalyzes the NAD^+-dependent oxidation of γ-GSA to yield glutamate (*1*−*3*).

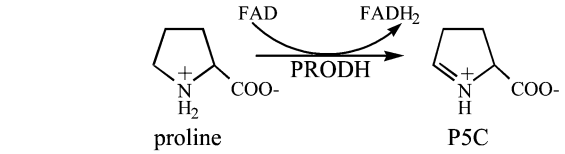

In addition to enzymatic functions, PutA is also an autogenous transcriptional regulator of proline utilization, respon-

† This research was supported in part by NSF Grant MCB0340912 and NIH Grant GM61068, the University of Nebraska Biochemistry Department and Redox Biology Center, and the Nebraska Agricultural Research Division, Journal Series No. 14559. This publication was also made possible by NIH Grant No. P20 RR-017675-02 from the National Center for Research Resources. Its contents are solely the responsibility of the authors and do not necessarily represent the official views of the NIH.

* Address correspondence to this author. E-mail: dbecker3@unl.edu. Phone: 402-472-9652. Fax: 402-472-7842.

[1] Abbreviations: FAD, flavin adenine dinucleotide; *put*, proline utilization; NAD^+, nicotinamide adenine dinucleotide; PRODH, proline dehydrogenase; P5CDH, Δ^1-pyrroline-5-carboxylate dehydrogenase; P5C, Δ^1-pyrroline-5-carboxylate; THFA, tetrahydro-2-furoic acid; DCPIP, dichlorophenolindophenol; EDTA, ethylenediaminetetraacetic acid; SDS−PAGE, sodium dodecyl sulfate−polyacrylamide gel electrophoresis; GSA, γ-glutamic acid semialdehyde; MES, 2-(*N*-morpholino)ethanesulfonic acid; TAPS, *N*-[tris(hydroxymethyl)methyl]-3-aminopropanesulfonic acid; PIPES, piperzaine-*N*,*N*′-bis(2-ethanesulfonic acid); HEPES, 4-(2-hydroxyethyl)piperazine-1-ethanesulfonic acid.

10.1021/bi051026b CCC: $30.25
Published on Web 08/25/2005

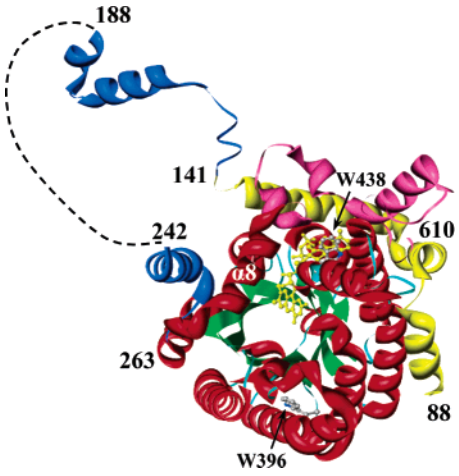

FIGURE 1: Modeling of the crystal structure of PutA86−669 complexed with L-lactate (1TJ1). Residue numbers are shown to indicate the different domains. The yellow domain (88−140) is a helical arm that wraps around the β/α barrel. The blue domain consists of residues 141−262 and contains regions that are poorly resolved. The dashed curve indicates the disordered residues (188−241) that are not observed in the structure including W194 and W211. Limited proteolysis studies have also shown that the blue domain contains highly flexible regions, namely, residues 215−235. The β/α barrel is shown in green/red (residues 263−561) with helix 8 labeled as α8. Helices positioned after the barrel are shown in purple. The FAD cofactor is highlighted in yellow, and also shown are residues W438 (top) and W396 (bottom). This illustration was drawn with UCSF Chimera (*30*).

sible for controlling expression of the *putA* and *putP* genes which are transcribed in opposite directions (*2*, *4*−*7*). The *putP* gene product is the high-affinity Na^+/proline transporter (*8*).

PutA from *E. coli*, the subject of this study, purifies predominantly as a dimer with a molecular mass of ∼293 kDa and one FAD molecule per subunit (*2*). The proposed organization of the functional domains in PutA is based on primary sequence analysis, molecular dissection, and three-dimensional structures. The DNA-binding domain of PutA is located in N-terminal residues 1−47 and most likely is a ribbon−helix−helix motif (*9*). X-ray crystal structures (2.0−2.1 Å) of a truncated PutA protein containing residues 86−669 (PutA86−669) bound with the competitive inhibitors L-lactate (K_i = 1.4 mM), acetate (K_i = 30 mM), and L-tetrahydro-2-furoic acid (THFA) (K_i = 0.2 mM) have provided a structural framework for the PRODH active site (*10*, *11*). Figure 1 shows a ribbon drawing of PutA86−669 complexed with L-lactate. The PRODH domain includes residues 263−610 and is comprised of a $\beta_8\alpha_8$ barrel with the FAD bound at the carboxyl termini of the β-strands of the barrel. Also, residues 88−140 form a three-α-helix arm that packs tightly against one side of the barrel, while residues 141−262 form a domain of unknown function that includes a three-helix bundle and a poorly resolved region, namely, residues 188−241 (*11*). The P5CDH domain is predicted by primary sequence analysis to include residues 650−1130 while the location of the membrane-binding domain appears to involve residues at the C-terminal region (*12*, *13*).

The regulation of *put* genes is dependent on the availability of proline and involves PutA intracellular compartmentalization. In the absence of proline, PutA accumulates in the cytoplasm and represses transcription of the *putA/P* genes by binding to the *put* control intergenic region (*2*, *7*, *14*). In the presence of proline, transcription of the *put* genes is activated by the movement of PutA to the cytoplasmic membrane where it performs the oxidation of proline (*15*−*17*). Proline appears to have little influence on PutA−DNA-binding affinity; however, proline significantly promotes PutA−membrane associations (*14*, *16*, *18*−*20*). Recently, the impact of ligand binding and FAD reduction on PutA−membrane associations was determined by kinetic measurements of PutA binding to model lipid bilayers using surface plasmon resonance (*20*). Nonreducing ligands such as L-THFA were observed to stimulate PutA−membrane binding, but the membrane-binding affinity generated by proline and FAD reduction was >300-fold greater, demonstrating that FAD reduction drives PutA−membrane binding (*20*). Thus, the regulation of PutA intracellular location and function is redox-based as first proposed by Wood (*15*). The increase in PutA−membrane binding affinity coincides with a proline-dependent conformational change (*19*, *21*). Limited proteolysis of PutA revealed that proline and FAD reduction induce protease susceptibility near R234 which is in the poorly structurally resolved region near the PRODH active site (*21*). Nonreducing ligands such as L-THFA also generate a new protease site near S216 (*21*). Therefore, perturbations in the PRODH domain such as ligand binding or FAD reduction trigger conformational transitions in a nearby flexible domain. However, similar to how FAD reduction generates greater membrane-binding affinity relative to nonreducing ligands, controlled potentiometric proteolysis has demonstrated that FAD reduction is the chief determinant of PutA conformational changes (*21*).

The X-ray crystal structure of PutA86−669 and previous proteolysis studies of full-length PutA indicate that the region involving residues 188−241 is flexible and is involved in conformational transitions that are necessary for switching PutA from a DNA-binding protein to a membrane-bound enzyme (*10*, *21*). Here, we seek to exploit W194 and W211 in this region and develop intrinsic Trp fluorescence as a spectroscopic tool for investigating the redox regulation of PutA structure and function. Intrinsic Trp fluorescence is an extremely useful probe for reporting protein conformational dynamics as shown in the recent study of the tetracycline repressor and the well-characterized dihydrofolate reductase from *E. coli* (*22*, *23*). In this study, we use a truncated form of PutA containing residues 86−601 (PutA86−601) which was designed to mimic the known structural region of PutA (88−610) and has been previously characterized (*24*). Wild-type PutA86−601 has comparable steady-state parameters and FAD redox properties to PutA, purifies as a monomer, and as anticipated lacks DNA-binding activity (*24*). PutA86−601 was chosen for this study because it contains only four Trp residues: W396 and W438 in the PRODH domain and W194 and W211 in the flexible domain. As shown in Figure 1, W396 is between α3 and β4 of the $\beta_8\alpha_8$ barrel while W438 stacks against the adenine of the FAD cofactor in the PRODH active site. W194 and W211, however, are located in the flexible domain previously identified by limited proteolysis, suggesting that these residues are effectively positioned to report on conformational changes in PutA. Consistent with this model, the Trp fluorescence of wild-type PutA86−601 decreases by 36% upon the addition of the substrate proline. Stopped-flow kinetic measurements show that the maximum rate for proline reduction of the FAD

cofactor is >200-fold faster than the observed rate of decrease in Trp fluorescence, consistent with the PRODH active site mediating the proline-induced quenching of Trp fluorescence. Replacement of W194 and W211 with Phe by site-directed mutagenesis reveals that W211 is the main reporter of the proline-induced conformational change in PutA86−601.

MATERIALS AND METHODS

Materials. All chemicals and buffers were purchased from Fisher Scientific and Sigma-Aldrich, Inc. Bicinchoninic acid (BCA) reagents used for protein quantitation were obtained from Pierce. *E. coli* strains XL-Blue and BL21(DE3) pLysS were purchased from Novagen. The vector pET23b (Stratagene) was used for expression of full-length PutA and the truncated PutA proteins as C-terminal 6×His-tagged proteins (*24*). Sequence-specific synthetic oligonucleotides for site-directed mutagenesis were purchased from Integrated DNA Technologies.

Preparation and Purification of Truncated Wild-Type PutA and Mutant Proteins. Initially in this work, the truncated PutA protein used for the steady-state fluorescence measurements and the site-directed mutagenesis studies was PutA86−601. Later, however, another truncated PutA protein containing residues 86−630 (PutA86−630) was used for the stopped-flow kinetic studies, which was originally designed to facilitate crystallization studies. PutA86−630 has 29 additional C-terminal residues but still has only four Trp residues. Steady-state fluorescence measurements of PutA86−630 show that Trp fluorescence decreases in the presence of proline by the same amount as that observed with PutA86−601. Thus, conclusions from the rapid reaction kinetics with PutA86−630 can be applied to the steady-state data described for PutA86−601.

PutA86−630 was prepared from the PutAΔ85 construct in pET23b (*9*). A *Bam*HI site was incorporated at amino acid codon 631 of the *putAΔ85* gene. *Bam*HI digestion then removed the corresponding PutA amino acid codons 631−1320, resulting in PutA86−630. The PutA86−630 construct in pET23b was confirmed by nucleic acid sequencing. The mutants W194F, W211F, and W194F/W211F were engineered in PutA86−601 in pET23b using QuickChange site-directed mutagenesis and the following oligonucleotides: W194F, 5′-CAGCAACGGTAACTTTCAGTCACACATTGGTCGTAGC-3′, and W211F, 5′-GTTAATGCCGCCACCTTTGGGCTGCTGTTTACTGGC-3′, and the corresponding complement for each oligonucleotide. All of the mutant constructs were confirmed by nucleic acid sequencing.

Full-length PutA and PutA86−601 were purified as described previously (*21*, *24*). Truncated PutA86−630 and mutant PutA86−601 proteins were overexpressed as C-terminal 6×His-tagged fusion proteins in *E. coli* strain BL21-(DE3) pLysS under the control of the T7 promoter as described previously except that expression was induced with IPTG at 25 °C for 3 h (*24*). Purification of the proteins followed a protocol previously described for PutA86−601 using Ni^{2+} NTA affinity chromatography (Novagen) (*24*). After elution from the Ni^{2+} NTA affinity column, fractions containing PRODH activity were pooled, incubated with a 10-fold molar excess of FAD, and then dialyzed overnight at 4 °C in 50 mM potassium phosphate (pH 7.3) containing 10% glycerol and 2 mM EDTA. Free FAD was then completely removed from the protein preparations by applying the protein−FAD mixtures onto a Bio-Gel P6 column (Bio-Rad) equilibrated with 50 mM potassium phosphate (pH 7.0) containing 10% glycerol and 1 mM EDTA. PutA proteins were concentrated using an Amicon ultrafiltration cell with 30 kDa molecular mass cutoff, frozen in liquid nitrogen, and stored at −70 °C. The C-terminal 6×His tag was retained after purification of each protein. The purity of each protein was estimated to be above 95% as judged by SDS−PAGE analysis (data not shown).

The concentration of each PutA protein was determined by the BCA method and spectrophotometrically using the estimated molar extinction coefficients of the main FAD absorption band near 450 nm for wild-type PutA86−601 and each Trp mutant (see Table 2). The molar extinction coefficients were estimated as previously described by precipitating each protein with 5% trichloroacetic acid (TCA) and quantitating the amount of released FAD using the molar extinction coefficient of 11.3 mM^{-1} cm^{-1} at 445 nm for free FAD (*13*). The reported molar extinction coefficients for wild-type PutA86−601 and the Trp mutants in Table 2 are the average values from two independent determinations. The molar ratio of FAD to wild-type PutA86−601 and the mutant polypeptides was assessed by comparing the total amount of released FAD to the total amount of denatured polypeptide as described previously (*13*).

Steady-State Kinetic Measurements. Michaelis−Menten parameters (K_m and V_{max}) for PRODH activity of wild-type PutA86−601 and mutants W194F, W211F, and W194F/W211F were determined in 100 mM MOPS buffer (pH 8.0) at 25 °C by varying proline concentration. PRODH activity was measured using dichlorophenolindophenol (DCPIP) as a terminal electron acceptor and phenazine methosulfate as a mediator (proline:DCPIP oxidoreductase assay) as previously described (*14*). One unit of PRODH activity is the quantity of enzyme that transfers electrons from 1 μmol of proline to DCPIP per minute at 25 °C. Assays were initiated by adding enzyme and were performed in triplicate. The kinetic parameters K_m and k_{cat} were estimated by linear regression analysis of the initial reaction velocity vs proline concentration using the Michaelis−Menten equation and Lineweaver−Burk plot analysis (*25*).

Fluorescence and UV−Visible Spectroscopic Measurements. Steady-state fluorescence studies were performed at room temperature in a Perkin-Elmer LS 50B spectroscope (Perkin-Elmer), fitted with a 450 W xenon arc lamp, using 6 nm slits for both excitation and emission. A 1 cm excitation and emission path length quartz cell was used for all of the fluorescence measurements. The intrinsic Trp fluorescence of each protein was measured by recording the emission spectra from 300 to 500 nm with a fixed excitation wavelength of 295 nm and averaging three scans. For measuring FAD fluorescence, emission spectra were recorded from 480 to 580 nm with a fixed excitation wavelength of 450 nm. For each experiment, protein was diluted to a final concentration of 1 μM in 3 mL of 50 mM potassium phosphate buffer (pH 7.5) with 10% glycerol. Fluorescence quenching experiments were performed by adding proline or THFA to the protein solution at a final concentration of 5 mM, equilibrating for 5 min, and then recording the Trp and FAD emission spectra. Spectra were corrected for

dilution after each experiment. UV−visible titrations of PutA86−601 with proline were performed as described (*14*). The titration data were analyzed as previously described assuming the formation of a reduced PutA−P5C complex (eq 1) (*14*, *19*).

$$\mathrm{PutA_{ox}} + \mathrm{proline} \leftrightarrow \mathrm{PutA_{red}{-}P5C} \quad (1)$$

The effect of pH on the fluorescence properties of wild-type PutA86−601 and its mutants W194F, W211F, and W194F/W211F was determined at room temperature from pH 5.8 to pH 9.5 using a mixed buffer system in place of the potassium phosphate buffer and consisted of 20 mM each of MES, HEPES, TAPS, and PIPES. As before, each protein was diluted to a final concentration of 1 μM in 3 mL of mixed buffer equilibrated at different pH values. The pH of each sample was measured before and after the experiment, and the average pH value was reported. The pH dependence of the fluorescence for oxidized wild-type PutA86−601 and the mutant W194F was fit to eqs 2 and 3, respectively, where FI_{obs} is the observed relative fluorescence intensity and ΔFI is the change in fluorescence intensity. Equation 2 describes a single ionization with a limit at low pH (FI_{lim}), and eq 3 describes two ionizations with limits at low pH (FI_{lim1}) and an intermediate plateau region (FI_{lim2}).

$$FI_{obs} = FI_{lim} + [(\Delta FI \times 10^{pH-pK_a})/(1 + 10^{pH-pK_a})] \quad (2)$$

$$FI_{obs} = (FI_{lim1} \times 10^{pH} + 10^{-pK_{a1}} FI_{lim2})/(10^{pH} + 10^{-pK_{a1}}) + [(10^{-pK_{a2}} \Delta FI)/(10^{pH} + 10^{-pK_{a2}})] \quad (3)$$

Stern−Volmer fluorescence quenching experiments were performed by adding 0.01−0.2 M acrylamide to 1 μM oxidized or proline-reduced wild-type PutA86−601 and mutants W194F, W211F, and W194F/W211F in 50 mM KP_i buffer and 10% glycerol, pH 7.5. The Trp fluorescence was measured as described above. The Stern−Volmer equation (eq 4) was used to analyze the quenching of the Trp fluorescence in which F_0 and F are the fluorescence intensities in the absence and presence of the quencher, [Q] is the concentration of the quencher, acrylamide, and K_{sv} is the Stern−Volmer quenching constant (eq 4).

$$F_0/F = 1 + K_{sv}[Q] \quad (4)$$

Rapid Reaction Kinetics. Stopped-flow multiple wavelength absorption studies were performed on an Applied Photophysics spectrophotometer (SX.MV18) equipped with a photodiode array detector and X-SCAN software (Applied Photophysics Ltd.). The temperature of the mixing chamber was maintained at 25 ± 1 °C and was controlled by a circulating water bath. The absorption spectra of the mixed solution were scanned in the range of 300−700 nm. In single wavelength studies, proline reduction of FAD was followed by monitoring the decrease in absorbance at 451 nm. Stopped-flow measurements of Trp fluorescence emission at >320 nm were monitored using an excitation wavelength of 295 nm and a cutoff filter to block fluorescence signals <320 nm. In the stopped-flow experiments, full-length PutA, PutA86−630, and substrate solutions were equilibrated in 50 mM phosphate buffer, pH 7.5. The stopped-flow reactions were initiated by mixing the enzyme with an equal volume of substrate. The reported concentrations of enzyme and substrate in the stopped-flow experiments are after mixing. The dependence of the rate of FAD reduction and Trp fluorescence quenching on proline concentration was determined by varying proline concentration from 0 to 700 mM. Observed rate constants were obtained by fitting the data with either a single-exponential or a double-exponential equation using nonlinear least-squares regression and Spectrakinetics software. The average of 10 individual reaction transients was used for the data analysis in each experiment. The apparent k_{max} and K_d for proline reduction of the FAD cofactor were determined by fitting the data to eq 5, where k_{obs} and k_{max} are the observed and maximum apparent rate constants, respectively, X is the concentration of proline, and K_d is the dissociation constant of the enzyme−substrate complex (eq 5).

$$k_{obs} = k_{max} X/(K_d + X) \quad (5)$$

RESULTS

Proline-Induced Changes in Trp Fluorescence. In previous studies, full-length PutA was shown by limited proteolysis to undergo distinct ligand- and redox-dependent conformational changes (*21*). Both reduction of the flavin and ligand binding cause increased proteolytic susceptibility in a region toward the N-terminus containing residues 215−235. Nonreducing ligands such as L-THFA also increase protease susceptibility in the C-terminal region around residues 1080−1100. To further explore the FAD-dependent conformational changes near the PRODH domain, we studied the small construct PutA86−601 by fluorescence spectroscopy. Because PutA86−601 contains only four Trp residues compared to full-length PutA, which contains 13 Trp residues, the intrinsic Trp fluorescence signal should disclose information about conformational changes in PutA86−601. To test whether proline induces intrinsic fluorescence changes, Trp fluorescence was recorded before and after the addition of proline (5 mM) to PutA86−601, which at 5 mM fully reduces the FAD cofactor. As shown in Figure 2 (panel A), proline quenched the intrinsic Trp fluorescence in PutA86−601 by ~36% at pH 7.5. The emission maximum (λ_{Emax}) of the Trp fluorescence signal, however, did not change, indicating that the average microenvironment of the Trp residues remained relatively constant upon the addition of proline (see Table 1). As anticipated, the fluorescence signal at 525 nm (excitation wavelength at 450 nm) from the FAD cofactor in PutA86−601 is also quenched by proline, indicating binding of proline to the active site and reduction of FAD (data not shown). Equilibrium constants of 4.2 and 5.1 mM^{-1} proline were estimated for the quenching of Trp and FAD fluorescence in PutA86−601 by titrating the enzyme with proline (Figure 3). Also shown in Figure 3 is a proline titration of the FAD cofactor in PutA86−601 followed by UV−visible spectroscopy. Reduction of the FAD cofactor as observed by the decrease in absorbance at 451 nm is characterized by an equilibrium constant of 4.3 mM^{-1} proline which matches that determined for Trp fluorescence quenching (Figure 3). Therefore, the observed Trp fluorescence quenching in PutA86−601 by proline must be due to a conformational change mechanism involving the FAD-binding site. In addition, adding proline to PutA86−

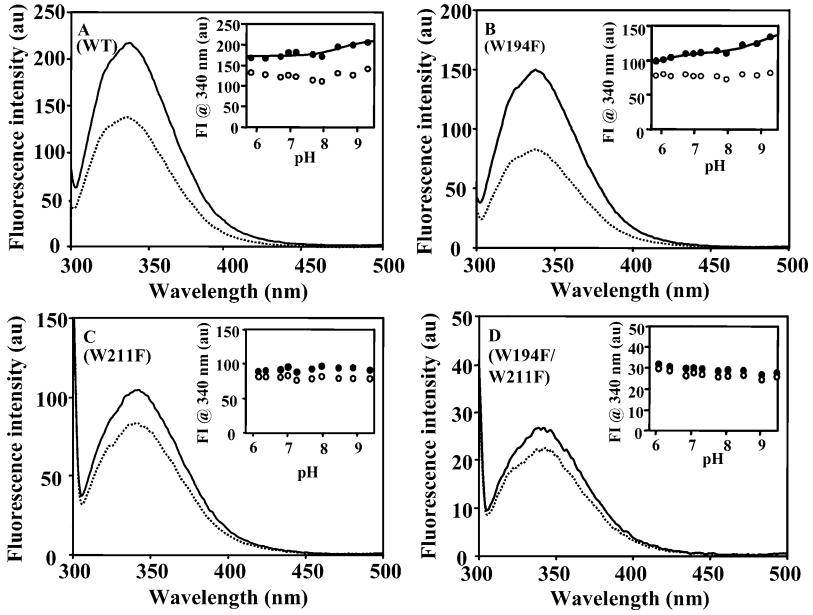

FIGURE 2: Fluorescence emission spectra of wild-type PutA86−601 (panel A) and mutants W194F (panel B), W211F (panel C), and W194F/W211F (panel D). These emission spectra were each recorded at 1 μM concentration in the absence (solid line) and presence (broken line) of 5 mM proline in 50 mM potassium phosphate buffer (pH 7.5) using $\lambda_{ex} = 295$ nm. Insets: Fluorescence pH profiles of wild-type PutA86−601 and mutants W194F, W211F, and W194F/W211F in the absence (solid circles) and presence (open circles) of proline. The fluorescence emission intensity (FI) of each PutA86−601 protein (1 μM) was measured at 340 nm using $\lambda_{ex} = 295$ nm in a mixed buffer system containing 20 mM each of MES, PIPES, TAPS, and HEPES from pH 5.8 to pH 9.5 at 23 °C. For wild-type PutA86−601 and mutant W194F the data from the plot of FI vs pH were fit to eqs 2 and 3, respectively, to yield a pK_a value of 8.5 ± 0.4 for wild-type PutA86−601 and pK_a values of 6.0 ± 0.6 and 9.0 ± 0.3 for W194F.

Table 1: Fluorescence Properties of Wild-Type PutA86−601 and Trp Mutants

enzyme	relative fluorescence intensity (RFI)	emission wavelength max (λ_{Emax}) (nm) −Pro	+Pro	% decrease in Trp fluorescence (ΔF_{340nm}) with Pro	ratio of Trp to FAD fluorescence decrease $\Delta F_{340}/\Delta F_{525}$
wild type	100	338	337	36	19.2
W194F	69	337.5	337.5	45	17.6
W211F	48	342.5	341	20	9.3
W194F/ W211F	13	338.5	338	17	9.5

601 apoprotein induces <5% decrease in Trp fluorescence relative to the holoprotein, demonstrating that the FAD cofactor is necessary for the conformational change observed by Trp fluorescence.

To determine whether substrate binding induces fluorescence quenching, PutA86−601 was titrated with L-THFA, a nonreducing proline analogue. Figure 3 shows that L-THFA binding to PutA86−601 also quenches Trp fluorescence with an equilibrium constant of 5.0 mM^{-1}. The decrease in Trp fluorescence elicited by L-THFA is approximately 35% and shows that both ligand binding and proline reduction of the FAD cofactor contribute to the observed proline-induced changes in Trp fluorescence, consistent with earlier limited proteolysis studies of full-length PutA which showed that L-THFA binding and FAD reduction increase proteolytic susceptibility in the same domain (*21*).

Stopped-Flow Kinetics. To further characterize the observed Trp fluorescence change in the presence of proline, rapid reaction kinetics coupled with UV−visible and fluorescence spectroscopy were performed to assess the rates of flavin reduction and Trp fluorescence quenching, respectively. Proline reduction of FAD under rapid reaction conditions was first characterized for full-length PutA. Figure 4 shows the photodiode array scans from 300 to 700 nm of FAD reduction in PutA by 100 mM proline. These are the first stopped-flow kinetic traces reported for PutA and show that no semiquinone intermediate is formed during proline reduction of PutA, consistent with a hydride transfer mechanism (*10*). An averaged observed rate constant of 7.6 ± 3.1 s^{-1} from 10 reaction transients was determined for proline (100 mM) reduction of the FAD cofactor in PutA by monitoring the decrease in absorbance at 451 nm (Figure 4, inset). Next, proline reduction of FAD in the truncated construct PutA86−630 was characterized in order to compare rates of FAD reduction with rates of Trp fluorescence changes. For these rapid reaction kinetic studies PutA86−630 was used instead of PutA86−601. Multiple wavelength scans of PutA86−630 upon mixing with proline showed a profile of FAD reduction similar to that observed for full-length PutA (Figure 4), indicating no significant changes in the mechanism of FAD reduction by proline (data not shown). The observed rate constant for FAD reduction (ΔA_{451nm}) in PutA86−630 by proline (100 mM) was estimated to be 57.6 ± 4.8 s^{-1} (Figure 5A), which is about 7-fold higher than PutA at the same proline concentration. The faster rate constant for FAD reduction observed with PutA86−630 is consistent with the higher steady-state turnover number for PutA86−630 (25 s^{-1}) relative to PutA (7.5 s^{-1}) (*13*). The rate of FAD reduction in PutA86−630 was also investigated under different proline concentrations as shown in Figure 6. The rate of FAD reduction displays a hyperbolic dependence on proline concentration (Figure 6). From the fit analysis a limiting rate constant for FAD reduction in PutA86−630 was estimated to be 132.5 ± 5.9

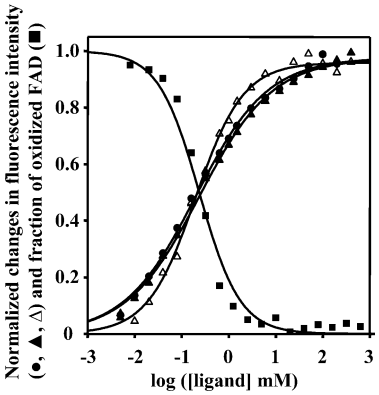

FIGURE 3: Proline and L-THFA titrations of wild-type PutA86−601 monitored by fluorescence and UV−visible spectroscopy. The effect of proline (▲) and L-THFA (●) on Trp fluorescence (λ_{ex} = 295 nm, λ_{em} = 340 nm) and proline (△) on FAD fluorescence (λ_{ex} = 450 nm, λ_{em} = 525 nm) was analyzed by plotting the normalized change in fluorescence intensity ($\Delta FI_{obs}/\Delta FI_{tot}$) vs log concentration (mM) of proline or L-THFA. Fluorescence emission was recorded at 340 nm (λ_{ex} = 295 nm) for wild-type Put86−601 (1 μM) during titrations with proline (0−600 mM) and L-THFA (0−600 mM) in 50 mM potassium phosphate buffer with 10% glycerol (pH 7.5) at 23 °C. The protein solution was allowed to equilibrate for 5 min after each proline or L-THFA addition prior to recording the fluorescence intensity. Reduction of the FAD cofactor by proline in PutA86−601 (12.9 μM) was monitored by recording the UV−visible spectrum of PutA86−601 after each addition of proline and measuring the decrease in absorbance at 451 nm. The normalized fraction of the oxidized FAD cofactor remaining [1 − ($\Delta Abs_{obs}/\Delta Abs_{tot}$)] after each addition of proline (■) is plotted vs log proline concentration (mM). Best-fit analysis of the proline titration data was performed assuming the formation of a reduced PutA−P5C complex while the L-THFA titration data were fit to a single-site binding isotherm. Equilibrium constants estimated from the best fits are 4.2 and 5.1 mM^{-1} proline for the changes in Trp and FAD fluorescence, respectively, 4.3 mM^{-1} proline for the reduction of the FAD cofactor monitored at 451 nm, and 5.0 mM^{-1} L-THFA for the changes in Trp fluorescence induced by L-THFA.

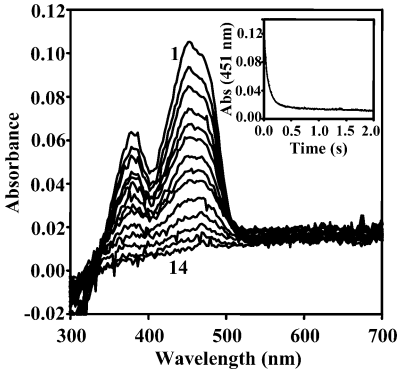

FIGURE 4: Rapid reaction kinetics of PutA with proline in 50 mM potassium phosphate buffer, pH 7.5, at 25 °C. PutA (10 μM) and proline (100 mM) were rapidly mixed and monitored by stopped-flow multiwavelength absorption using a photodiode array detector and X-scan software (Applied Photophysics Ltd.). The first spectrum was recorded at 1.3 ms after the initial mixing event, and the subsequent reaction was monitored for 25 s. For clarity, only selected spectra are shown. Curves 1−14: 0.0013, 0.0525, 0.104, 0.155, 0.257, 0.308, 0.411, 0.557, 0.751, 1.010, 2.370, 4.190, 5.510, and 12.68 s. Inset: Typical stopped-flow kinetic trace of the change in absorbance at 451 nm upon rapidly mixing PutA (10 μM) with proline (100 mM) in 50 mM potassium phosphate buffer at pH 7.5. The solid line is the best fit of the experimental data to a double-exponential model. The rate constants obtained from the fitting are k_{obs1} = 9.8 ± 0.2 s^{-1} (87% amplitude) and k_{obs2} = 1.05 ± 0.04 s^{-1} (13% amplitude).

s^{-1} with a dissociation constant (K_d) of 114.6 ± 17.3 mM proline. These results show that FAD reduction is not rate limiting during steady-state turnover.

Next, the rate of the Trp fluorescence quenching was determined for PutA86−630. No decrease in Trp fluorescence was observed upon mixing PutA86−630 with buffer alone (Figure 5B, curve 1). Figure 5B (curve 2) shows the trace of fluorescence changes at >320 nm ($\Delta F_{>320nm}$) for PutA86−630 with 100 mM proline. An apparent rate constant of 0.59 ± 0.06 s^{-1} for the decrease in Trp fluorescence was determined from the fit analysis. The observed rate constant for Trp quenching is nearly 100-fold slower relative to FAD reduction at 100 mM proline, indicating that FAD reduction precedes the observed decrease in Trp fluorescence. Furthermore, Figure 6 shows that the rate of Trp fluorescence quenching in PutA86−630 is independent of proline concentration from 2.5 to 700 mM proline, which demonstrates that the observed fluorescence change in PutA86−630 is a much slower process relative to FAD reduction and that FAD reduction is not rate-limiting in the conformational change. The amplitude of the fluorescence change was also constant over this range of proline concentration.

Spectroscopic and Steady-State Kinetic Properties of PutA86−601 Trp Mutants. To determine which Trp residues are involved in the observed fluoresence decrease and conformational change, W194 and W211 in PutA86−601 were replaced by Phe residues in the mutants W194F, W211F, and the double mutant W194F/W211F. W194 and W211 were chosen because these residues are in the region of PutA (residues 188−241) where increased protease susceptibility was detected in the presence of proline. Furthermore, the other two Trp residues, W396 and W438, are located in the PRODH domain, and W438 is clearly involved in FAD binding (see Figure 1). The UV−visible spectra and kinetic properties of wild-type PutA86−601 and the PutA86−601 mutants W194F, W211F, and W194F/W211F are shown in Figure 7 and summarized in Table 2. No significant changes in the UV−visible spectra of the PutA86−601 mutants W194F, W211F, and W194F/W211F were observed relative to wild-type PutA86−601 except for relatively higher molar extinction coefficients at 375 and 449 nm in the mutant W194F/W211F. The molar extinction coefficients of the main FAD absorbance band for the PutA86−601 proteins ranged from 12.9 to 15.0 $mM^{-1}cm^{-1}$ (Table 2). All of the mutants generally exhibited lower FAD incorporation (around 0.5−0.6 mol/mol of polypeptide) relative to that of wild-type PutA86−601 (0.8 mol of FAD/mol of polypeptide). The steady-state kinetic parameters for wild-type PutA86−601 and the mutant proteins are also summarized in Table 2. Each of the Trp mutants has a K_m value comparable to that of wild-type PutA86−601; however, the k_{cat} values are lower, especially for the PutA86−601 mutant W194F/W211F, which has a k_{cat} value that is about 40-fold lower than wild-type PutA86−601. From these data, it appears that the W211F mutation has the largest impact on k_{cat}.

The intrinsic Trp fluorescence spectra of the PutA86−601 mutants W194F, W211F, and W194F/W211 are shown in Figure 2 (panels B−D) and summarized in Table 1. The emission spectra of the oxidized wild-type PutA86−601 and

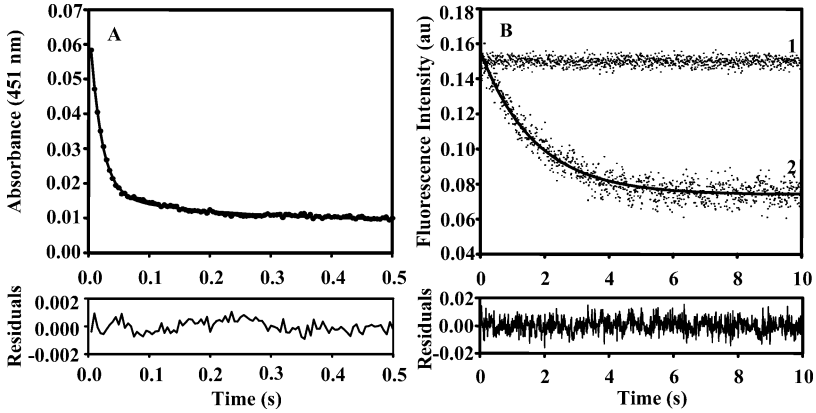

FIGURE 5: Rapid reaction kinetics of proline-dependent reduction of FAD and Trp fluorescence changes in PutA86−630. Panel A: Stopped-flow kinetic trace of the change in absorbance at 451 nm upon rapidly mixing PutA86−630 (10 μM) with proline (100 mM) in 50 mM potassium phosphate buffer, pH 7.5, at 25 °C. The solid line is a best fit of the experimental data to a double-exponential model. The rate constants obtained from the fitting are $k_{obs1} = 53.8 \pm 6.1$ s^{-1} (88% amplitude) and $k_{obs2} = 4.8 \pm 2.4$ s^{-1} (12% amplitude). The distribution of the residuals from the fit is shown below. Panel B: (Curve 1) Stopped-flow kinetic trace of Trp fluorescence emission >320 nm following the rapid mixing of PutA86−630 (10 μM) with 50 mM potassium phosphate buffer (pH 7.5) alone. (Curve 2) Stopped-flow kinetic trace of the changes in Trp fluorescence >320 nm upon mixing PutA86−630 (10 μM) with proline (100 mM) in 50 mM potassium phosphate buffer, pH 7.5, at 25 °C. The experimental data were fit to a single-exponential decay model with $k_{obs} = 0.59 \pm 0.06$ s^{-1}. The distribution of the residuals from the fit is shown below.

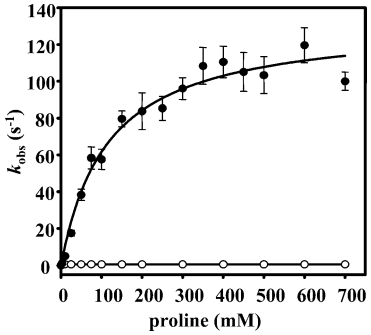

FIGURE 6: Dependence of the observed rate constant (k_{obs}) for FAD reduction (●) and changes in Trp fluorescence (○) of PutA86−630 on proline concentration. Put86−630 (10 μM) was mixed with varying concentrations of proline (0−700 mM) in 50 mM potassium phosphate buffer (pH 7.5) at 25 °C, and the changes in UV−visible absorbance and fluorescence emission were monitored at 451 nm and >320 nm, respectively. The rate constants at the different proline concentrations were determined from theoretical double-exponential fits of the decrease in absorbance at 451 nm and single-exponential fits of the change in Trp fluorescence. (●) The average rate constant from 10 kinetic traces for the decrease in absorbance at 451 nm, k_{obs1}, plotted vs proline concentration. The data are fit to eq 5 to yield a limiting rate constant of 133 ± 6 s^{-1} for proline reduction of FAD and a dissociation constant (K_d) of 114.6 ± 17.3 mM proline. (○) The average rate constant from 10 kinetic traces for the decrease in Trp fluorescence plotted vs proline concentration.

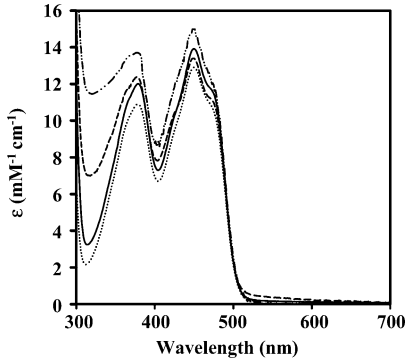

FIGURE 7: UV−visible spectra of wild-type PutA86−601 and Trp mutant proteins. The UV−visible spectra of wild-type PutA86−601 (—), W194F (• • •), W211F (- - -), and W194F/W211F (- • • -) were each recorded at a concentration of 10 μM in 50 mM potassium phosphate buffer, pH 7.5, at 23 °C.

Table 2: Spectroscopic and Kinetic Properties of Wild-Type PutA86−601 and Trp Mutant Enzymes[a]

	λ_{max} (nm)		ϵ_λ (mM^{-1} cm^{-1})		K_m	k_{cat}	k_{cat}/K_m
enzyme	1	2	1	2	(mM)	(s^{-1})	(s^{-1} M^{-1})
wild type[b]	379	451	10.6	13.9	58 ± 5	20 ± 0.6	345
W194F	376	450	10.6	12.9	56 ± 6	10 ± 0.4	179
W211F	377	449	11.9	13.4	59 ± 9	4 ± 0.2	68
W194F/W211F	375	449	12.8	15.0	32 ± 4	0.5 ± 0.02	16

[a] Parameters were estimated by best-fit analysis to the Michaelis−Menten equation. [b] Values from ref *21*.

mutant enzymes shown in Figure 2 exhibit broad fluorescence emission maxima (λ_{Emax}) ranging from 337.5 to 342.5 nm. A 4.5 nm red shift in λ_{Emax} was observed in the mutant W211F relative to wild-type PutA86−601, indicating that W211 may have a slightly more hydrophobic microenvironment than the average environment of all the Trp residues. The fluorescence intensity of the PutA86−601 mutants W194F, W211F, and W194F/W211F relative to wild-type PutA86−601 clearly shows a disproportionate contribution to the intrinsic Trp fluorescence by W211. The decrease in relative fluorescence intensity by the W211F substitution indicates that W211 contributes ~50% of the total fluorescence signal. The mutants W194F and W194F/W211F were characterized by relative fluorescence intensities that are diminished by 31% and 87%, respectively, relative to wild-type PutA86−601 (Figure 2). The nearly abolished Trp fluorescence of the PutA86−601 mutant W194F/W211F demonstrates that W396 and W438 contribute weakly to the overall relative intrinsic Trp fluorescence and that fluorescence from these Trp residues is significantly quenched by interactions in the protein such as W438 with the adenine moiety of the FAD cofactor.

Proline-induced fluorescence quenching of the PutA86−601 Trp mutants was then characterized by steady-state

fluorescence measurements in the presence of 5 mM proline, at which concentration proline fully reduces the FAD cofactor in each of the mutant proteins. Figure 2 shows that, in the mutants W194F, W211F, and W194F/W211F, proline induces relative decreases in fluorescence intensity of 45%, 20%, and 17%, respectively. Because the mutant proteins vary somewhat in FAD incorporation, we also evaluated the ratio of the decrease in Trp fluorescence to FAD fluorescence ($\Delta F_{340}/\Delta F_{525}$) to compare the impact of each Trp mutation on proline-dependent fluorescence changes. As summarized in Table 1, the ratios of $\Delta F_{340}/\Delta F_{525}$ for wild-type PutA86−601 and W194F are similar with values of 19.2 and 17.6, respectively. However, the $\Delta F_{340}/\Delta F_{525}$ values for the mutants W211F and W194F/W211F are 2-fold lower. Thus, W211 appears to be mainly responsible for the observed fluorescence quenching and therefore is the primary marker of the FAD-dependent conformational change in PutA86−601.

Although proline induces a substantial decrease in fluorescence intensity, no shift in λ_{Emax} was observed for wild-type PutA86−601, W194F, W211F, and W194F/W211F upon the addition of proline, indicating that the overall microenvironments of the Trp residues do not change (see Table 1). To test whether any changes in solvent accessibility accompany proline reduction of FAD, we measured the quenching of Trp fluorescence by acrylamide in wild-type PutA86−601 and mutants W194F and W211F (*26*). The Stern−Volmer constants (K_{sv}) for acrylamide quenching of Trp fluorescence were fairly high for the oxidized enzymes, ranging from 7.94 M^{-1} (wild-type), 6.93 M^{-1} (W194F), and 7.14 M^{-1} (W211F) with only slight changes (± 1 M^{-1}) in K_{sv} values observed in the presence of proline (data not shown). Thus, significant changes in solvent accessibility do not account for the observed proline quenching of Trp fluorescence.

Effect of pH on Trp Fluorescence. The observation that the proline-induced decrease in fluorescence intensity of wild-type PutA86−601, W194F, and W211F was not due to solvent accessibility changes or alterations in the polarity of the microenvironment suggests that Trp fluorescence is quenched by another mechanism perhaps involving a side-chain group of a nearby residue. In an attempt to identify pH-sensitive quenching groups, we measured Trp fluorescence of oxidized and proline-reduced wild-type PutA86−601, W194F, W211F, and W194F/W211F as a function of pH ranging from 5.8 to 9.5. The insets to Figure 2 show the pH dependence of the Trp fluorescence intensity for each protein in the absence and presence of proline. In the oxidized state, the fluorescence intensity of wild-type PutA86−601 and W194F generally increases at the higher pH values by 10−20% while the intrinsic fluorescence of W211F and W194F/W211F is basically pH independent. The pH-dependent increase in the intrinsic fluorescence of oxidized wild-type PutA86−601 and the mutant W194F is described by pK_a values of 8.5 ± 0.4 and 9.0 ± 0.3, respectively. In the presence of proline, all of the proteins exhibit pH-independent Trp fluorescence. The weak pH profile of PutA86−601 fluorescence indicates that the quenching mechanism does not involve a clear pH-dependent component. However, the different pH profiles of Trp fluorescence for the oxidized mutants W194F and W211F do ascribe the slight pH sensitivity of PutA86−601 fluorescence to W211.

DISCUSSION

Proline availability governs whether PutA functions as a DNA-binding protein or a membrane-bound enzyme. The mechanism by which proline promotes PutA−membrane binding is redox-based, involving a global conformational change in the enzyme (*15*, *20*, *21*). To further characterize conformational transitions in PutA and to develop a spectroscopic tool for analyzing how changes in the PRODH active site are transmitted out of the FAD-binding domain, we explored the intrinsic Trp fluorescence properties of PutA. Intrinsic fluorescence studies with the full-length PutA polypeptide (144 kDa) are not feasible due to the presence of 13 Trp residues and proline inducing only about a 10% decrease in Trp fluorescence (data not shown). From previous limited proteolysis studies, however, it is evident that critical regions involved in the proline-dependent conformational change include the PRODH active site (residues 263−610) and a nearby flexible domain (141−262) of unknown function (*21*). Accordingly, a truncated PutA protein that contains both domains (i.e., PutA86−601 or PutA86−630) and only four Trp residues was used instead of full-length PutA to examine proline-dependent conformational changes by intrinsic Trp fluorescence. Proline elicited a 36% decrease in the Trp fluorescence of PutA86−601, indicating a substantial conformational change. The nonreducing ligand L-THFA also caused a similar decrease in Trp fluorescence, confirming that the PutA conformation is sensitive to both ligand binding and FAD reduction in the PRODH active site.

Site-directed mutagenesis was used to identify the main reporter group of the fluorescence changes in PutA86−601. The X-ray crystal structure of PutA86−669 shows that W396 and W438 are part of the active site $\beta_8\alpha_8$ barrel while W194 and W211 are located in a region that is not resolved in the structure (*11*). Because W194 and W211 are located in a flexible domain, we chose to make Phe substitutions at these positions. Steady-state fluorescence measurements of the PutA86−601 mutants W194F and W211F revealed important insights into the Trp fluorescence properties and structural transitions of PutA86−601. First, in the absence of proline, it is apparent that together W194 and W211 contribute over 80% of the total Trp fluorescence in PutA86−601. Clearly, the intrinsic fluorescence of W396 and W438 is substantially quenched. The fluorescence of W438, for example, is most likely decreased by interactions with the adenine moiety of FAD, which in the X-ray crystal structure of PutA86−669 is stacked upon the indole ring of W438 within <3.9 Å (*11*). A potentially strong quenching group of W396, however, is not readily apparent. Considering that W194 and W211 are responsible for most of the Trp fluorescence in PutA86−601, it seemed plausible that the conformational change observed by intrinsic fluorescence changes is reported by these residues. After examining the proline-dependent fluorescence changes of the mutants W194F and W211F, W211 was determined to be the primary reporting group. The W194F mutant has properties similar to wild-type PutA86−601 with a comparative $\Delta F_{340}/\Delta F_{525}$ ratio of ~18 while the W211F mutant displays a significantly diminished proline-dependent fluorescence change with a $\Delta F_{340}/\Delta F_{525}$ ratio of ~9. Thus, W211 is highly sensitive to proline binding and FAD reduction in the PRODH active site.

Scheme 1

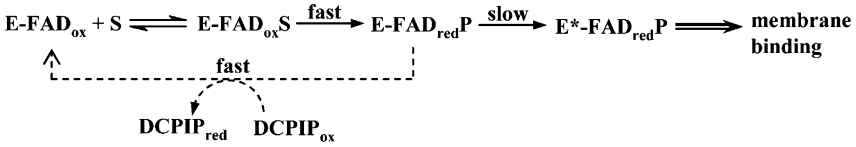

Apparently, changes in the microenvironment polarity and solvent accessibility of W211 do not accompany the conformational transition since negligible changes in the fluorescence emission wavelength or Stern−Volmer constants were observed in the presence of proline. Instead, the observed decrease in Trp fluorescence in the presence of proline may involve a quenching group from a nearby residue or a backbone amide. Studies have implicated amide groups as effective quenchers of Trp fluorescence via an electron transfer mechanism with the amide serving as the acceptor (*27*−*29*). In this case, local electric field effects can have a significant impact on whether an amide group will be an effective quencher (*28*, *29*). The presence of differently charged groups near the indole ring of Trp and the amide group strongly influences the charge transfer mechanism (*28*). Thus, the quenching of Trp fluorescence observed in the presence of proline could be due to a closer positioning of W211 with an amide acceptor group or a change in the local electric field that enhances charge transfer.

The apparent rate constant (k_{obs}) determined for the proline-dependent conformational change is about 10-fold slower than the turnover number for PRODH activity in PutA, indicating that the conformational change is not part of the catalytic cycle. Instead, it is part of a regulatory pathway that directs the association of PutA with the membrane. Scheme 1 illustrates that in proline:DCPIP oxidoreductase assays reoxidation of the reduced FAD cofactor occurs during steady-state turnover (7.5 s^{-1}) before the slower conformational change (0.59 s^{-1}; E−FAD$_{red}$P → E*−FAD$_{red}$P) can occur. Proline-reduced PutA reacts sluggishly with air ($t_{1/2}$ ∼ 120 min), and presumably ubiquinone is the physiological electron acceptor for PutA (*14*). Consequently, PutA is expected to remain in the proline-reduced state on a longer time scale in vivo, allowing for the slower structural transformation of PutA into the membrane-binding conformer (E*−FAD$_{red}$P). Once membrane-bound, PutA completes the catalytic cycle by transferring electrons from the reduced FAD cofactor to the electron transport chain system of *E. coli*. Thus, the conformational change is not only required for directing PutA to the membrane for transcriptional activation of the *put* genes but is also necessary to complete the oxidative half-reaction of the initial catalytic event. Once PutA is peripherally bound to the membrane, the conformational change is no longer necessary as most likely PutA remains membrane associated during subsequent turnovers. Therefore, the conformational change is only required for mediating the initial proline-dependent translocation of PutA.

Future work will exploit the intrinsic fluorescence properties of PutA86−630 to determine how the PRODH active site transmits signals to the nearby flexible domain, specifically W211. Analysis of PutA669 and PutA86−669 structures complexed with nonreducing ligands has provided some insights. For example, R556 which makes critical ion pair interactions with the carboxylate group of the substrate is located on the α8 helix of the $\beta_8\alpha_8$ barrel (*10*, *11*). The α8 helix appears to bridge the PRODH and flexible domains, thus potentially mediating ligand binding and conformational changes in PutA (see Figure 1). A residue that is well positioned to sense changes in the FAD redox state is R431 with the NH1 atom 2.9 Å from the N(5) position of the FAD (*10*). The impact of these residues on the kinetics of PutA conformational changes and membrane binding will be the focus of future studies.

ACKNOWLEDGMENT

We thank Dr. Javier Seravalli for help with the rapid reaction kinetic experiments and Berevan A. Baban for designing the PutA86−630 construct. The molecular graphics image was produced using the UCSF Chimera package from the Computer Graphics Laboratory, University of California, San Francisco (supported by NIH Grant P41 RR-01081).

REFERENCES

1. Abrahamson, J. L. A., Baker, L. G., Stephenson, J. T., and Wood, J. M. (1983) Proline dehydrogenase from *Escherichia* K12, properties of the membrane-associated enzyme, *Eur. J. Biochem. 134*, 77−82.
2. Brown, E., and Wood, J. M. (1992) Redesigned purification yields a fully functional PutA protein dimer from *Escherichia coli*, *J. Biol. Chem. 267*, 13086−13092.
3. Menzel, R., and Roth, J. (1981) Enzymatic properties of the purified *putA* protein from *Salmonella typhimurium*, *J. Biol. Chem. 256*, 9762−9766.
4. Wood, J. M. (1981) Genetics of L-proline utilization in *Eschericia coli*, *J. Bacteriol. 146*, 895−901.
5. Menzel, R., and Roth, J. (1981) Regulation of genes for proline utilization in *Salmonella typhimurium*: autogenous repression by the *putA* gene product, *J. Mol. Biol. 148*, 21−44.
6. Maloy, S., and Roth, J. R. (1983) Regulation of proline utilization in *Salmonella typhimurium*: characterization of *put*:Mu d(Ap, *lac*) operon fusions, *J. Bacteriol. 154*, 561−568.
7. Ostrovsky De Spicer, P., O'Brian, K., and Maloy, S. (1991) Regulation of proline utilization in *Salmonella typhimurium*: a membrane-associated dehydrogenase binds DNA *in vitro*, *J. Bacteriol. 173*, 211−219.
8. Chen, C.-C., and Wilson, T. H. (1986) Solubilization and functional reconstitution of the proline transport system of *Escherichia coli*, *J. Biol. Chem. 261*, 2599−2604.
9. Gu, D., Zhou, Y., Kallhoff, V., Baban, B., Tanner, J. J., and Becker, D. F. (2004) Identification and characterization of the DNA-binding domain of the multifunctional PutA flavoenzyme, *J. Biol. Chem. 279*, 31171−31176.
10. Lee, Y. H., Nadaraia, S., Gu, D., Becker, D. F., and Tanner, J. J. (2003) Structure of the proline dehydrogenase domain of the multifunctional PutA flavoprotein, *Nat. Struct. Biol. 10*, 109−114.
11. Zhang, M., White, T. A., Schuermann, J. P., Baban, B. A., Becker, D. F., and Tanner, J. J. (2004) Structures of the *Escherichia coli* PutA proline dehydrogenase domain in complex with competitive inhibitors, *Biochemistry 43*, 12539−12548.
12. Ling, M., Allen, S. W., and Wood, J. M. (1994) Sequence analysis identifies the proline dehydrogenase and pyrroline-5-carboxylate dehydrogenase domains of the multifunctional *Escherichia coli* PutA protein, *J. Mol. Biol. 245*, 950−956.
13. Vinod, M. P., Bellur, P., and Becker, D. F. (2002) Electrochemical and functional characterization of the proline dehydrogenase

domain of the PutA flavoprotein from *Escherichia coli*, *Biochemistry 41*, 6525−6532.
14. Becker, D. F., and Thomas, E. A. (2001) Redox properties of the PutA protein from *Escherichia coli* and the influence of the flavin redox state on PutA-DNA interactions, *Biochemistry 40*, 4714−4722.
15. Wood, J. (1987) Membrane association of proline dehydrogenase in *Escherichia coli* is redox dependent, *Proc. Natl. Acad. Sci. U.S.A. 84*, 373−377.
16. Muro-Pastor, A. M., Ostrovsky, P., and Maloy, S. (1997) Regulation of gene expression by repressor localization: biochemical evidence that membrane and DNA binding by the PutA protein are mutually exclusive, *J. Bacteriol. 179*, 2788−2791.
17. Surber, M. W., and Maloy, S. (1999) Regulation of flavin dehydrogenase compartmentalization: requirements for PutA-membrane association in *Salmonella typhimurium*, *Biochim. Biophys. Acta 1421*, 5−18.
18. Muro-Pastor, A. M., and Maloy, S. (1995) Proline dehydrogenase activity of the transcriptional repressor PutA is required for induction of the *put* operon by proline, *J. Biol. Chem. 270*, 9819−9827.
19. Brown, E. D., and Wood, J. M. (1993) Conformational change and membrane association of the PutA protein are coincident with reduction of its FAD cofactor by proline, *J. Biol. Chem. 268*, 8972−8979.
20. Zhang, W., Zhou, Y., and Becker, D. F. (2004) Regulation of PutA-membrane associations by flavin adenine dinucleotide reduction, *Biochemistry 43*, 13165−13174.
21. Zhu, W., and Becker, D. F. (2003) Flavin redox state triggers conformational changes in the PutA protein from *Escherichia coli*, *Biochemistry 42*, 5469−5477.
22. Kedracka-Krok, S., Gorecki, A., Bonarek, P., and Wasylewski, Z. (2005) Kinetic and thermodynamic studies of tet repressor-tetracycline interaction, *Biochemistry 44*, 1037−1046.
23. Rajagopalan, P. T., Zhang, Z., McCourt, L., Dwyer, M., Benkovic, S. J., and Hammes, G. G. (2002) Interaction of dihydrofolate reductase with methotrexate: ensemble and single-molecule kinetics, *Proc. Natl. Acad. Sci. U.S.A. 99*, 13481−13486.
24. Baban, B. A., Vinod, M. P., Tanner, J. J., and Becker, D. F. (2004) Probing a hydrogen bond pair and the FAD redox properties in the proline dehydrogenase domain of *Escherichia coli* PutA, *Biochim. Biophys. Acta 1701*, 49−59.
25. Lineweaver, H., and Burk, D. (1934) The determination of enzyme dissociation constants, *J. Am. Chem. Soc. 56*, 658−666.
26. Eftink, M. R., and Ghiron, C. A. (1976) Exposure of tryptophanyl residues in proteins. Quantitative determination by fluorescence quenching studies, *Biochemistry 15*, 672−680.
27. Chen, Y., Liu, B., Yu, H.-T., and Barkley, M. D. (1996) The peptide bond quenches indole fluorescence, *J. Am. Chem. Soc. 118*, 9271−9278.
28. Callis, P. R., and Liu, T. (2004) Quantitative prediction of fluorescence quantum yields for tryptophan in proteins, *J. Phys. Chem. B 108*, 4248−4259.
29. Nanda, V., and Brand, L. (2000) Aromatic interactions in homeodomains contribute to the low quantum yield of a conserved, buried tryptophan, *Proteins: Struct., Funct., Genet. 40*, 112−125.
30. Huang, C., Couch, G., Pettersen, E., and Ferrin, T. (1996) Chimera: an extensible molecular modeling application constructed using standard components, *Pac. Symp. Biocomput. '96 1*, 724.

BI051026B